

**Application of higher order decouplings of the dilated electron propagator to  $2\pi$  CO<sup>-</sup>,  $2\pi$  g N<sup>2-</sup> – and  $2\pi$  g C<sub>2</sub>H<sub>2</sub> – shape resonances**

S. Mahalakshmi, Arun Venkatnathan, and Manoj K. Mishra

Citation: *The Journal of Chemical Physics* **115**, 4549 (2001); doi: 10.1063/1.1394754

View online: <http://dx.doi.org/10.1063/1.1394754>

View Table of Contents: <http://scitation.aip.org/content/aip/journal/jcp/115/10?ver=pdfcov>

Published by the [AIP Publishing](#)

---

**Articles you may be interested in**

Electron induced reactions in molecular nanofilms of chlorodifluoroacetic acid (CCIF<sub>2</sub>COOH) : Desorption of fragment anions and formation of CO<sub>2</sub>

*J. Chem. Phys.* **133**, 194503 (2010); 10.1063/1.3505550

Complex absorbing potentials in the framework of electron propagator theory. II. Application to temporary anions

*J. Chem. Phys.* **118**, 6188 (2003); 10.1063/1.1557452

Higher order decouplings of the dilated electron propagator with applications to  $2p$  Be<sup>-</sup>,  $2p$  Mg<sup>-</sup> – shape and  $2s$  Be<sup>+</sup> ( $1s^{-1}$ ) Auger resonances

*J. Chem. Phys.* **114**, 35 (2001); 10.1063/1.1328395

Infrared spectra of the CO<sub>2</sub><sup>-</sup> and C<sub>2</sub>O<sub>4</sub><sup>-</sup> – anions isolated in solid argon

*J. Chem. Phys.* **110**, 2414 (1999); 10.1063/1.477947

Characterization of molecular shape resonances using different decouplings of the dilated electron propagator with application to  $2\pi$ CO<sup>-</sup> and  $2\pi$  B<sub>2</sub>g C<sub>2</sub>H<sub>4</sub> – shape resonances

*J. Chem. Phys.* **103**, 676 (1995); 10.1063/1.470101

---



# Application of higher order decouplings of the dilated electron propagator to ${}^2\Pi\text{CO}^-$ , ${}^2\Pi_g\text{N}_2^-$ and ${}^2\Pi_g\text{C}_2\text{H}_2^-$ shape resonances

S. Mahalakshmi,<sup>a)</sup> Arun Venkatnathan,<sup>b)</sup> and Manoj K. Mishra<sup>c)</sup>

Department of Chemistry, Indian Institute of Technology, Bombay Powai, Mumbai 400 076, India

(Received 14 May 2001; accepted 27 June 2001)

The full third order ( $\Sigma^3$ ), quasi-particle third order ( $\Sigma_q^3$ ) and outer valence Green's function (OVGF-A) decouplings of the bi-orthogonal dilated electron propagator have been implemented and results from their application to  ${}^2\Pi\text{CO}^-$ ,  ${}^2\Pi_g\text{N}_2^-$ , and  ${}^2\Pi_g\text{C}_2\text{H}_2^-$  shape resonances are presented and compared with energies and widths obtained using the zeroth order ( $\Sigma^0$ ), quasiparticle second order ( $\Sigma_q^2$ ) and second order ( $\Sigma^2$ ) decouplings. The energies and widths from the various  $\Sigma^3$  decouplings for shape resonances are close to those obtained using the  $\Sigma^2$  approximant but the corresponding Feynman–Dyson amplitudes (FDAs) differ considerably. The differences between FDAs from different decouplings are analyzed to elicit the role of correlation and relaxation in the formation and decay of shape resonances. © 2001 American Institute of Physics.

[DOI: 10.1063/1.1394754]

## I. INTRODUCTION

The electron propagator theory<sup>1,2</sup> has proved to be an accurate and versatile tool for the treatment of ionization energies and electron affinities.<sup>3–8</sup> The dilated<sup>9–11</sup> (complex scaled) electron propagator method,<sup>12–14</sup> where all the electronic coordinates have been scaled by a complex scale factor ( $\eta = \alpha e^{i\theta}$ ) has been quite effective in describing electron attachment shape and electron detachment Auger resonances.<sup>15</sup> In these calculations, the resonances are located by plotting the poles of the dilated electron propagator as a function of  $\alpha$  and  $\theta$  ( $\alpha$  and  $\theta$  trajectories) and those showing a semblance of invariance with respect to variations in  $\theta$  are associated with resonances.<sup>16</sup> This quest for stability necessitates that calculations be done for  $\sim 5–10\alpha$  and  $\sim 20–30\theta$  values (per  $\alpha$ ) and makes these calculations at least 100 times more demanding as compared to the real electron propagator calculations.

These computational difficulties had led to the use of second and pseudosecond order decouplings of the dilated electron propagator in the treatment of atomic and molecular resonances.<sup>15</sup> The advent of faster CPUs and large memory and storage however has made it possible recently to apply the full third order and related decouplings to the treatment of atomic shape and Auger resonances<sup>17</sup> and it is our purpose in this paper to present some results from first application of the third order decouplings to some prototypical molecular resonances.

The isoelectronic  ${}^2\Pi\text{CO}^-$ ,<sup>18,19–21</sup>  ${}^2\Pi_g\text{N}_2^-$ ,<sup>22–28</sup> and  ${}^2\Pi_g\text{C}_2\text{H}_2^-$  (Refs. 29–37) shape resonances typify metastable electron attachment to heteronuclear/homonuclear diatomic and simple nonpolar polyatomic molecules and have been

studied extensively both experimentally and computationally. These are our systems of choice as well. The formal expressions for the third order decouplings have been detailed in a previous paper<sup>17</sup> and only a brief outline of the methodology is offered in the next section. A discussion of results from our application using the outer valence Green's function ( $\Sigma_{\text{OVGF}}^3$ ), quasiparticle third order ( $\Sigma_q^3$ ), and full third order ( $\Sigma^3$ ) decouplings to the study of  ${}^2\Pi\text{CO}^-$ ,  ${}^2\Pi_g\text{N}_2^-$ , and  ${}^2\Pi_g\text{C}_2\text{H}_2^-$  shape resonances are offered in Sec. III and a summary of the main results in Sec. IV concludes this paper.

## II. METHOD

The Dyson equation for the dilated bi-orthogonal matrix electron propagator is similar to that of the undilated electron propagator and may be expressed<sup>15</sup> as

$$\mathbf{G}(\eta, \mathbf{E}) = (\tilde{\mathbf{a}} | (E\hat{I} - \hat{H}(\eta))^{-1} | \mathbf{a}), \quad (1)$$

where  $\{a_i\}$  represent the annihilation operators defined on orbitals  $\{\psi_i\}$  and  $\{\tilde{a}_j\}$  are the annihilation operators defined on bi-orthogonal orbitals  $\{\phi_j\}$ .<sup>14,38</sup> We define the identity superoperator  $\hat{I}$  and the Hamiltonian superoperator  $\hat{H}(\eta)$  by

$$\hat{I}X = X, \quad \hat{H}(\eta)X = [X, H(\eta)]_- \quad \forall X \in L, \quad (2)$$

where  $X$  is an element of the linear manifold of electron field operators  $L$ .<sup>39,40</sup> The scalar product on the manifold  $L$  (Ref. 41) is defined by

$$(X_i | X_j) = \langle N | [X_i^\dagger, X_j]_+ | N \rangle \quad \forall X, Y \in L \quad (3)$$

and the dilated Hamiltonian  $H(\eta)$  is given by

$$H(\eta) = H_0(\eta) + V(\eta) \quad \text{with} \quad H_0(\eta) = \sum_k \epsilon_k(\eta) \tilde{a}_k^\dagger a_k, \quad (4)$$

and

<sup>a)</sup>Present address: Department of Chemistry, Texas A&M University, College Station, Texas 77842-3012.

<sup>b)</sup>Present address: Department of Chemistry and Biochemistry, University of California, Los Angeles, California 90095-1569.

<sup>c)</sup>Electronic mail: mmishra@chem.iitb.ac.in

$$V(\eta) = \sum_{i'l'} \langle ii' || ll' \rangle [\frac{1}{4} \tilde{a}_i^\dagger \tilde{a}_i^\dagger a_l a_l - \delta_{i'l'} \langle n_{i'} \rangle \tilde{a}_i^\dagger a_l], \quad (5)$$

where the antisymmetric two-electron integral

$$\langle ij || kl \rangle = \eta^{-1} \int \psi_i(1) \psi_j(2) [(1 - P_{12})/r_{12}] \times \psi_k(1) \psi_l(2) dx_1 dx_2, \quad (6)$$

and the absence of complex conjugation on  $\psi_i$  and  $\psi_j$  stems from the bi-orthonormal sets of orbitals resulting from bi-variational SCF being the complex conjugate of each other  $\{\phi_i = \psi_i^*\}$ .<sup>38,43</sup>

Using a complete projection manifold,  $\mathbf{h} = \mathbf{a} \oplus \mathbf{f}$  of one electron operators, the dilated electron propagator [Eq. (1)] may be recast as<sup>15</sup>

$$\begin{aligned} \mathbf{G}^{-1}(\eta, E) &= (\tilde{\mathbf{a}} | (E\hat{I} - \hat{H}(\eta)) | \mathbf{a}) - (\tilde{\mathbf{a}} | \hat{H}(\eta) | \mathbf{f}) \\ &\quad \times (\tilde{\mathbf{f}} | (E\hat{I} - \hat{H}(\eta)) | \mathbf{f})^{-1} (\tilde{\mathbf{f}} | \hat{H}(\eta) | \mathbf{a}) \\ &= \mathbf{A}_0 + \mathbf{A} - \mathbf{B}\mathbf{C}^{-1}\mathbf{D}, \end{aligned} \quad (7)$$

where

$$\mathbf{A}_0 = (\tilde{\mathbf{a}} | (E\hat{I} - \hat{H}_0(\eta)) | \mathbf{a}), \quad \mathbf{A} = (\tilde{\mathbf{a}} | \hat{V}(\eta) | \mathbf{a}), \quad (9)$$

$$\mathbf{B} = (\tilde{\mathbf{a}} | \hat{H}(\eta) | \mathbf{f}), \quad \mathbf{D} = (\tilde{\mathbf{f}} | \hat{H}(\eta) | \mathbf{a}), \quad (10)$$

and

$$\mathbf{C} = (\tilde{\mathbf{f}} | (E\hat{I} - \hat{H}(\eta)) | \mathbf{f}). \quad (11)$$

$\mathbf{A}_0$  is the Hartree–Fock electron propagator in which the reference state  $|N\rangle$  is approximated by  $|\text{HF}\rangle$  and  $\mathbf{A}$ ,  $\mathbf{B}$ ,  $\mathbf{C}$ , and  $\mathbf{D}$  may be evaluated to desired orders in  $V(\eta)$ .

Our order analysis for the dilated electron propagator<sup>17</sup> is similar to that for real unscaled electron propagator<sup>2,42</sup> and proceeds by expressing the exact  $N$  electron reference state  $|N\rangle$  using a Rayleigh–Schrödinger perturbation expansion<sup>2</sup> with

$$|N\rangle = |\text{HF}\rangle + |0^1\rangle + |0^2\rangle + \dots, \quad (12)$$

where  $|\text{HF}\rangle$  is the Hartree–Fock ground state wave function and  $|0^1\rangle$  and  $|0^2\rangle$  are the first and second order Møller–Plesset corrections, respectively.

The contributions from the first order ( $\mathbf{A}_1$ ) and second order ( $\mathbf{A}_2$ ) energy independent terms are zero. The energy dependent terms in the self-energy matrix can be evaluated from  $\mathbf{B}\mathbf{C}^{-1}\mathbf{D}$ . In order to obtain the second order terms, we use the Hartree–Fock ground state to obtain  $\mathbf{B}$  and  $\mathbf{D}$  through first order. We separate  $\mathbf{C}$  into  $\mathbf{C}_0$  and  $\mathbf{C}_1$  such that  $\mathbf{C} = \mathbf{C}_0 - \mathbf{C}_1$ , where

$$\mathbf{C}_0 = (\tilde{\mathbf{f}} | (E\hat{I} - \hat{H}_0(\eta)) | \mathbf{f}) \quad \text{and} \quad \mathbf{C}_1 = (\tilde{\mathbf{f}} | \hat{V}(\eta) | \mathbf{f}). \quad (13)$$

If one retains only  $\mathbf{f} = \{\mathbf{h}_3\} = \{a_k^\dagger a_l a_m, \dots\}$  and approximates  $|N\rangle$  by  $|\text{HF}\rangle$  this expansion is terminated in zeroth order and one obtains the second order ( $\Sigma^2$ ) self-energy term  $\Sigma^2(E) = \mathbf{B}_1\mathbf{C}_0^{-1}\mathbf{D}_1$  given by

$$\begin{aligned} \Sigma_{ij}^2(\eta, E) &= \frac{1}{2} \left[ \sum_a \sum_b \sum_p \frac{\langle ip || ab \rangle \langle ab || jp \rangle}{E + \epsilon_p - \epsilon_a - \epsilon_b} \right. \\ &\quad \left. + \sum_a \sum_p \sum_q \frac{\langle ia || pq \rangle \langle pq || ja \rangle}{E + \epsilon_a - \epsilon_p - \epsilon_q} \right], \end{aligned} \quad (14)$$

where the indices  $a, b, c, d$  denote the occupied,  $p, q, r, s$  the unoccupied and  $i, j, k, l$  the unspecified orbitals. Similarly, diagonal 2ph-TDA decoupling<sup>44,45</sup> of the dilated electron propagator<sup>46</sup> is given by

$$\begin{aligned} \Sigma_{ij}^{2ph-TDA}(\eta, E) &= \frac{1}{2} \left[ \sum_a \sum_b \sum_p \frac{\langle ip || ab \rangle \langle ab || jp \rangle}{E + \epsilon_p - \epsilon_a - \epsilon_b - \Delta_1} \right. \\ &\quad \left. + \sum_a \sum_p \sum_q \frac{\langle ia || pq \rangle \langle pq || ja \rangle}{E + \epsilon_a - \epsilon_p - \epsilon_q - \Delta_2} \right], \end{aligned} \quad (15)$$

where

$$\Delta_1 = -\frac{1}{2} \langle ab || ab \rangle + \langle bp || bp \rangle + \langle ap || ap \rangle,$$

$$\Delta_2 = \frac{1}{2} \langle pq || pq \rangle - \langle aq || aq \rangle - \langle ap || ap \rangle,$$

except that the transformed two electron integrals and the orbital energies obtained from the bi-variational SCF are complex.

Contributions to third order terms of  $A$  arise from the first order double excitation and second order single excitation configurations in the Rayleigh–Schrödinger expansion of the ground state wave function and the third order energy dependent part of the dilated self-energy matrix once again<sup>2,17,47</sup> emerges as

$$\Sigma_{ED}^3(\eta, E) = \mathbf{B}_2\mathbf{C}_0^{-1}\mathbf{D}_1 + \mathbf{B}_1\mathbf{C}_0^{-1}\mathbf{D}_2 + \mathbf{B}_1\mathbf{C}_0^{-1}\mathbf{C}_1\mathbf{C}_0^{-1}\mathbf{D}_1, \quad (16)$$

where the subscript ED denotes energy-dependent self-energy matrix and implicit dependence of all terms in Eq. (16) on  $\eta$  has been suppressed.

The third order energy independent dilated self-energy is also formally similar to the real undiluted electron propagator formulas,<sup>47</sup> i.e.,

$$[\Sigma_{\text{EI}}^3(\eta)]_{ij} = \sum_k \sum_l \langle ik || jl \rangle \gamma_{kl}, \quad (17)$$

with

$$\gamma_{kl} = \langle N | k^\dagger l | N \rangle. \quad (18)$$

Using  $|N\rangle = |\text{HF}\rangle + |0^1\rangle + |0^2\rangle$  we generate the third order energy independent self-energy matrix, which is

$$\begin{aligned} [\Sigma_{\text{EI}}^3(\eta)]_{ij} &= \sum_k \sum_l \langle ik || jl \rangle \langle 0^1 | k^\dagger l | 0^1 \rangle \\ &\quad + \sum_k \sum_l \langle ik || jl \rangle \langle 0^2 | k^\dagger l | \text{HF} \rangle \\ &\quad + \sum_k \sum_l \langle ik || jl \rangle \langle \text{HF} | k^\dagger l | 0^2 \rangle. \end{aligned} \quad (19)$$

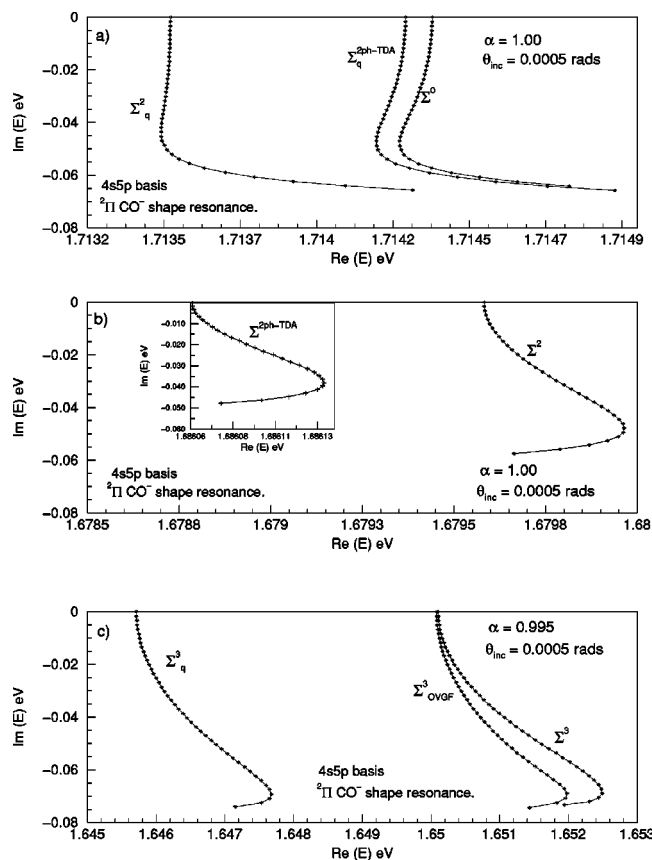


FIG. 1. Theta trajectories from different decouplings of dilated electron propagator calculations on the  ${}^2\Pi$   $\text{CO}^-$  shape resonance. The trajectories start on the real line ( $\theta=0.0$ ) and  $\theta$  increments are in steps ( $\theta_{\text{inc}}$ ) of 0.0005 rad.

The outer valence Green's function (OVGF) (Refs. 3, 7) approximation is based on full third order approximation to  $\Sigma$  and also contains a geometric approximation for higher order contributions. No matrices need to be diagonalized. Since  $\Sigma^2$  corrections are nonzero and large we have utilized the OVGF-A (Ref. 7) decoupling in our calculations.

In terms of the spin-orbitals obtained from the bivariational SCF procedure, combining Eqs. (7) and (8) we may write the matrix electron propagator as

$$\mathbf{G}^{-1}(\eta, E) = \mathbf{A}_0 + \mathbf{A} - \mathbf{B}\mathbf{C}^{-1}\mathbf{D} = \mathbf{E}\mathbf{I} - \epsilon(\eta) - \Sigma(\eta, E) = \mathbf{E}\mathbf{I} - \mathbf{L}(\eta, E) \quad (20)$$

or in operator form,

$$\hat{G}(\eta, E) = [E\hat{I} - \hat{L}(\eta, E)]^{-1}, \quad (21)$$

whereby in terms of the eigenfunctions and eigenvalues of  $L(\eta, E)$ ,

$$L(\eta, E) \chi_n(\eta, E) = \mathcal{E}_n(\eta, E) \chi_n(\eta, E). \quad (22)$$

The spectral representation of  $G$  is given by

$$G(\eta, E) = [E - L(\eta, E)]^{-1} \sum_n |\chi_n\rangle\langle\chi_n| = \sum_n \frac{|\chi_n\rangle\langle\chi_n|}{E - \mathcal{E}_n(\eta, E)} \quad (23)$$

TABLE I. Energy and width of the  ${}^2\Pi$   $\text{CO}^-$  shape resonance.

| Method   | Energy (eV) | Width (eV) |
|--|-------------|------------|
| Experiment <sup>a</sup>  | 1.50        | 0.40       |
| Theoretical approaches:  |             |            |
| Boomerang model <sup>b</sup>   | 1.52        | 0.80       |
| T matrix method <sup>c</sup>   | 3.40        | 1.65       |
| Close coupling method <sup>d</sup>   | 1.75        | 0.28       |
| Second order dilated electron Propagator (real SCF) <sup>e</sup>                                 | 1.71        | 0.08       |
| Results from bi-orthogonal dilated Electron propagator (this work):                              |             |            |
| Zeroth order ( $\Sigma^0$ ), quasiparticle   | 1.71        | 0.10       |
| Second order ( $\Sigma_q^2$ ) and quasiparticle Diagonal 2ph-TDA ( $\Sigma_q^{2\text{ph-TDA}}$ ) | 1.68        | 0.09       |
| Second order ( $\Sigma^2$ ) Diagonal 2ph-TDA ( $\Sigma^{2\text{ph-TDA}}$ )                       | 1.69        | 0.08       |
| Quasi-particle third order ( $\Sigma_q^3$ )  | 1.65        | 0.14       |
| OVGF third order ( $\Sigma_{\text{OVGF}}^3$ )  | 1.65        | 0.14       |
| Third order ( $\Sigma^3$ )/( $\Sigma^3$ ) <sup>f</sup>   | 1.65/1.65   | 0.14/0.14  |

<sup>a</sup>Reference 22.

<sup>b</sup>Reference 19.

<sup>c</sup>Reference 20.

<sup>d</sup>Reference 21.

<sup>e</sup>Reference 50.

<sup>f</sup>Single point  $\Sigma^3(\eta, E)$  calculation for  $\eta = \eta_{\text{opt}}^q$  and  $E = E_{\text{res}}^q$  obtained from  $\Sigma_q^3$  calculations.

and the eigenvalues of  $L$  therefore represent the poles of  $G$ . Accordingly, the usual dilated electron propagator calculations proceed by iterative diagonalization,

$$\mathbf{L}(\eta, E) \chi_n(\eta, E) = \mathcal{E}_n(\eta, E) \chi_n(\eta, E) \quad (24)$$

with

$$\mathbf{L}(\eta, E) = \epsilon(\eta) + \Sigma(\eta, E), \quad (25)$$

where  $\epsilon(\eta)$  is the diagonal matrix of orbital energies obtained from a bivariational complex SCF (Refs. 38, 43) and  $\Sigma$  is the self-energy matrix. The propagator pole  $\mathcal{E}$  is obtained by repeated diagonalizations such that one of the eigenvalues  $\mathcal{E}_n(\eta, E)$  of  $\mathbf{L}(\eta, E)$  fulfills the condition  $E = \mathcal{E}_n(\eta, E)$ .<sup>15</sup> These  $\mathcal{E}_n(\eta, E)$  represent the poles of the dilated electron propagator  $G(\eta, E)$ . From among these poles, the resonant pole  $\mathcal{E}_r(\eta, E)$  and the corresponding eigenvector (FDA)  $\chi_r(\eta, E)$  are selected as per the prescription of the complex scaling theorems,<sup>10,11</sup> whereby those roots in the continua which are invariant to changes in the complex scaling parameter  $\eta$  are to be associated with resonances. In a limited basis set calculation, instead of absolute stability one finds quasistability where the  $\theta$  trajectory displays kinks, cusps, loops or inflections which indicate the proximity of a stationary point<sup>16</sup> and in our case the resonance attributes have been extracted from the value at the inflection points in  $\theta$ -trajectories. The real part of the resonant pole furnishes the energy and the imaginary part the half width of the resonance.

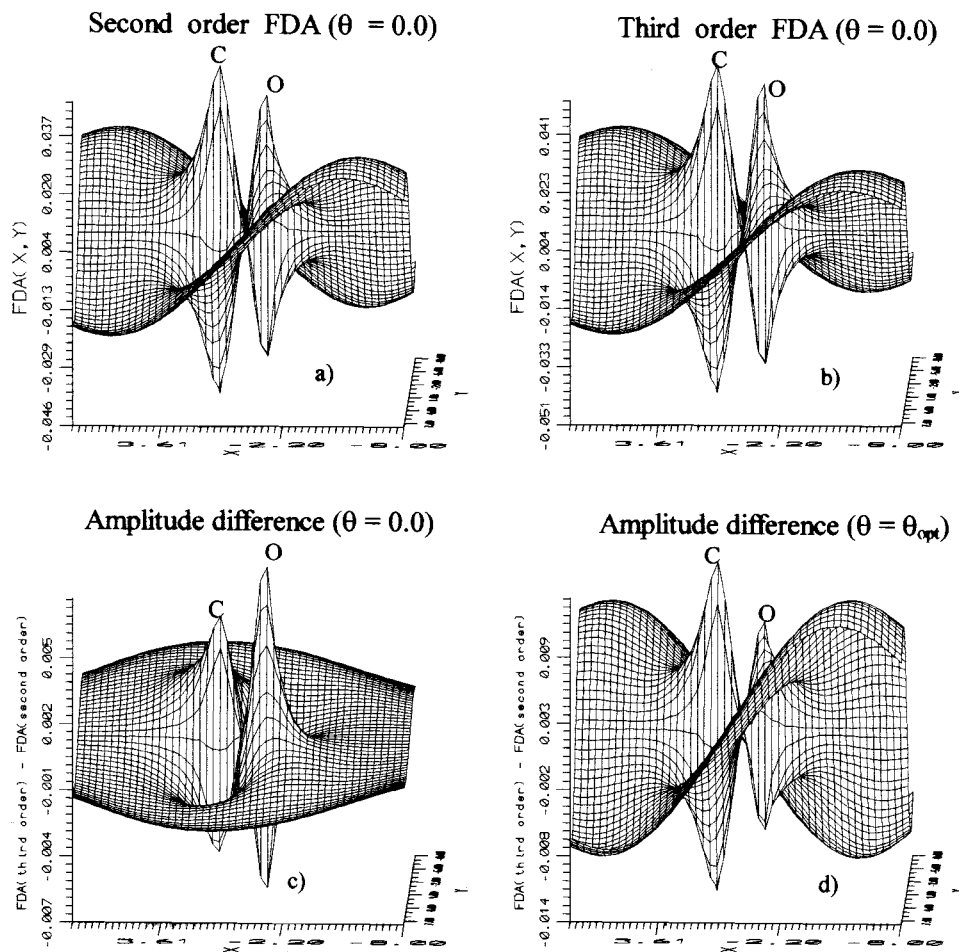


FIG. 2. The FDAs for  $\Sigma^2$  and  $\Sigma^3$  decoupling and difference between the resonant FDAs from the second and third order decoupling at  $\theta=0.0$  and between the real parts at  $\theta=\theta_{\text{opt}}$  for  ${}^2\Pi$   $\text{CO}^-$  shape resonance are plotted in (a), (b), (c), and (d), respectively.

The quasiparticle approximation<sup>48</sup> for dilated electron propagator<sup>49</sup> results from a diagonal approximation to the self-energy matrix  $\Sigma(\eta, E)$  with poles of the dilated electron propagator given by

$$E(\eta) = \epsilon_i(\eta) + \Sigma_{ii}(\eta, E), \quad (26)$$

which are determined iteratively beginning with  $E = \epsilon_i$  and  $\Sigma_{ii}$  may correspond to any perturbative ( $\Sigma^2$ ) or renormalized decoupling like the diagonal  $\Sigma^{2\text{ph-TDA}}$ .

In the bivariationally obtained biorthogonal orbital basis  $\{\psi_i\}$ , the FDA  $\chi_n$  is a linear combination,

$$\chi_n(\mathbf{r}) = \sum_i C_{ni} \psi_i(\mathbf{r}), \quad (27)$$

where the mixing of the canonical orbitals allows for the incorporation of correlation and relaxation effects. In the zeroth ( $\Sigma=0$ ) and quasiparticle approximations (diagonal  $\Sigma$ ), there is no mixing. The difference between perturbative second/third order ( $\Sigma^2/\Sigma^3$ ) or renormalized diagonal 2ph-TDA ( $\Sigma^{2\text{ph-TDA}}$ ) decouplings manifests itself through differences between the mixing coefficients  $C_{ni}$  from these approximations.

### III. RESULTS AND DISCUSSION

The isoelectronic systems  ${}^2\Pi$   $\text{CO}^-$ ,  ${}^2\Pi_g$   $\text{N}_2^-$ , and  ${}^2\Pi_g$   $\text{C}_2\text{H}_2^-$  represent the simplest heteronuclear/homonuclear diatomic and nonpolar polyatomic shape resonances and

have been routinely used to assess the effectiveness of experimental and theoretical procedures in eliciting qualitative and quantitative details of molecular shape resonances. The earlier investigation of these resonances using the second order and related decouplings of the dilated electron propagator<sup>15,29</sup> provided resonance energies in good agreement with the experimental results but the quality of the

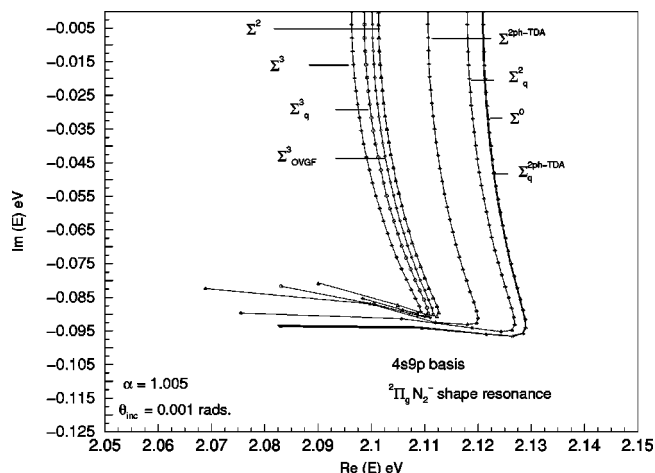


FIG. 3. Theta trajectories from different decouplings of dilated electron propagator calculations on the  ${}^2\Pi_g$   $\text{N}_2^-$  shape resonance. The trajectories start on the real line ( $\theta=0.0$ ) and  $\theta$  increments are in steps ( $\theta_{\text{inc}}$ ) of 0.001 rad.

TABLE II. Energy and width of the  ${}^2\Pi_g N_2^-$  shape resonance.

| Method  | Energy (eV) | Width (eV) |
|---|-------------|------------|
| Experiment <sup>a</sup>   | 2.20        | 0.57       |
| Theoretical approaches:   |             |            |
| Static exchange <sup>b</sup>  | 3.70        | 1.16       |
| Static exchange $R$ -matrix <sup>c</sup>  | 2.15        | 0.34       |
| Stabilization method <sup>d</sup>   | 2.44        | 0.32       |
| $R$ -Matrix <sup>c</sup>  | 3.26        | 0.80       |
| Many-body optical potential <sup>f</sup>  | 3.80        | 1.23       |
| Boomerang model <sup>g</sup>  | 1.91        | 0.54       |
| Stieltjes imaging technique <sup>h</sup>  | 4.13        | 1.14       |
| Complex SCF <sup>i</sup>  | 3.19        | 0.44       |
| Second order dilated electron Propagator (real SCF) <sup>j</sup>                          | 2.14        | 0.26       |
| Results from bi-orthogonal dilated Electron propagator (this work):                       |             |            |
| Zeroth order ( $\Sigma^0$ ), quasiparticle  | 2.12        | 0.19       |
| Second order ( $\Sigma_q^2$ ) and quasiparticle Diagonal 2ph-TDA ( $\Sigma_q^{2ph-TDA}$ ) |             |            |
| Second order ( $\Sigma^2$ )   | 2.11        | 0.18       |
| Diagonal 2ph-TDA ( $\Sigma^{2ph-TDA}$ )   | 2.12        | 0.18       |
| Quasi-particle/OVGF third order ( $\Sigma_q^3/\Sigma_{OVGF}^3$ )                          | 2.11        | 0.18       |
| Third order ( $\Sigma^3$ )/( $\Sigma^3$ ) <sup>k</sup>                                    | 2.11/2.11   | 0.18/0.18  |

<sup>a</sup>Reference 18.<sup>b</sup>Reference 23.<sup>c</sup>Reference 24.<sup>d</sup>Reference 25.<sup>e</sup>Reference 26.<sup>f</sup>References 27 and 28.<sup>g</sup>Reference 55.<sup>h</sup>Reference 56.<sup>i</sup>Reference 57.<sup>j</sup>Reference 58.<sup>k</sup>Single point  $\Sigma^3(\eta, E)$  calculation for  $\eta = \eta_{opt}^q$  and  $E = E_{res}^q$  obtained from the  $\Sigma_q^3$  calculation.

calculated widths is difficult to ascertain due to lack of sufficient experimental data for impact energy independent width. Our values for the width of these resonances has been narrower in comparison to those from other theoretical techniques. It is therefore useful to apply the  $\Sigma_{OVGF}^3$ ,  $\Sigma_q^3$ , and  $\Sigma^3$  decouplings to these prototypical resonances to ascertain the effectiveness of these higher order decouplings and the results from our application of these various third order decouplings to  ${}^2\Pi CO^-$ ,  ${}^2\Pi_g N_2^-$ , and  ${}^2\Pi_g C_2H_2^-$  are presented below.

### A. The ${}^2\Pi CO^-$ shape resonance

The primitive basis set used for the investigation of  ${}^2\Pi CO^-$  shape resonance is that used earlier in second order dilated electron propagator calculations<sup>50,51</sup> with a  $4s5p$  CGTO basis centered on C and another  $4s5p$  CGTO basis centred on O.<sup>50</sup> The  $\theta$ -trajectories for the resonance root from  $\Sigma^0$ ,  $\Sigma^2$ ,  $\Sigma_q^{2ph-TDA}$ ,  $\Sigma^{2ph-TDA}$ ,  $\Sigma^2$ ,  $\Sigma_{OVGF}^3$ ,  $\Sigma_q^3$ , and  $\Sigma^3$  decouplings of the dilated electron propagator are displayed in Fig. 1. Third order calculation has also been done by constructing, iterating, and diagonalizing the full third order  $\Sigma^3(\eta_{opt}^q, E_{res}^q)$  dilated electron propagator for a single optimal  $\eta = \eta_{opt}^q$  and  $E = E_{res}^q$  (the resonant pole at  $\eta_{opt}^q$ ) obtained from the quasistable portion of the  $\Sigma_q^3$   $\theta$ -trajectory which we designate as the  $\Sigma^3$  approximant. The near identity between

the full  $\Sigma^3$  and  $\Sigma^3$  results suggests that  $\Sigma^3$  is a viable alternative to obtain accurate resonant poles and FDAs. The energy and width obtained from the quasistable portion of these  $\theta$  trajectories along with the experimental results and those from other theoretical techniques are collected in Table I. The resonance energy obtained from all the dilated electron propagator decouplings employed here are in reasonably good agreement with the experimental result, with higher order decouplings offering marginal improvement. The incorporation of  $\Sigma^3$  decouplings does decrease the energy and increase the width but our calculated widths are much narrower in comparison to those from other techniques. A comparison with energies and widths from second and third order decouplings shows that the much more (by  $\sim n^2$  factor, where  $n$  is the number of basis functions) demanding third order decoupling gives energies and widths which are almost the same as that obtained from the second order decoupling. As seen in Table I, the different third order decouplings like the OVGF ( $\Sigma_{OVGF}^3$ ), quasiparticle third order ( $\Sigma_q^3$ ) and full third order (both  $\Sigma^3$  and  $\Sigma^3$ ) give similar values for both the resonance energies and widths. The much more economic quasiparticle decouplings which require the computation of only one  $\Sigma_{ii}$  element and no iterative construction as opposed to  $[n^*(n+1)/2]\Sigma_{ij}$  elements followed by iterative diagonalization thereby afford great savings and recommend themselves for economic and effective investigation of resonances, more so since similar effectiveness of the quasiparticle decouplings has been demonstrated in real electron propagator calculation as well.<sup>52</sup> The diagonal decouplings however provide no mixing of the SCF orbitals and the corresponding FDAs are therefore devoid of correlation and relaxation effects. This has prompted us to obtain the resonance attributes by constructing the  $\Sigma^3(\eta, E)$  matrix for a single  $\eta = \eta_{opt}^q$  and single  $E = E_{res}^q$  elicited from the quasistable portion of the  $\Sigma_q^3$   $\theta$ -trajectory and since this approximation ( $\Sigma^3$ ) is much more economic and offers results almost identical to those from the full  $\Sigma^3$  implementation, we feel that this is a desirable alternative to the full  $\Sigma^3$  approximation.

The third order decoupling is further tested by plotting the  $\Sigma^2$  and  $\Sigma^3$  FDAs at  $\theta=0.0$  and the difference between  $\Sigma^3$  and  $\Sigma^2$  Feynman–Dyson amplitudes at  $\theta=0.0$  and  $\theta = \theta_{opt}$  in Fig. 2. The individual FDAs from the  $\Sigma^2$  and  $\Sigma^3$  decouplings are indeed the  $\pi^*$  LUMO with more amplitude on carbon than on oxygen and establish the utility of the dilated electron propagator method in unequivocal identification of LUMOs as the resonant FDA. The difference between the second and the third order FDAs at  $\theta=0.0$  is plotted in Fig. 2(c) and shows that  $\Sigma^3$  decoupling provides more amplitude on both the carbon and oxygen atoms but the accumulation of electron density is more on oxygen as compared to carbon. This diminution in the antibonding character of the CO  $\pi^*$  LUMO on the real line is remedied by complex scaling since the difference between FDAs from second and third order decouplings at  $\theta = \theta_{opt}$  as displayed in Fig. 2(d) shows that the amplitude accumulation is reversed with greater amplitude on C than on O. Also, the third order decoupling provides larger amplitude on both C and O atoms

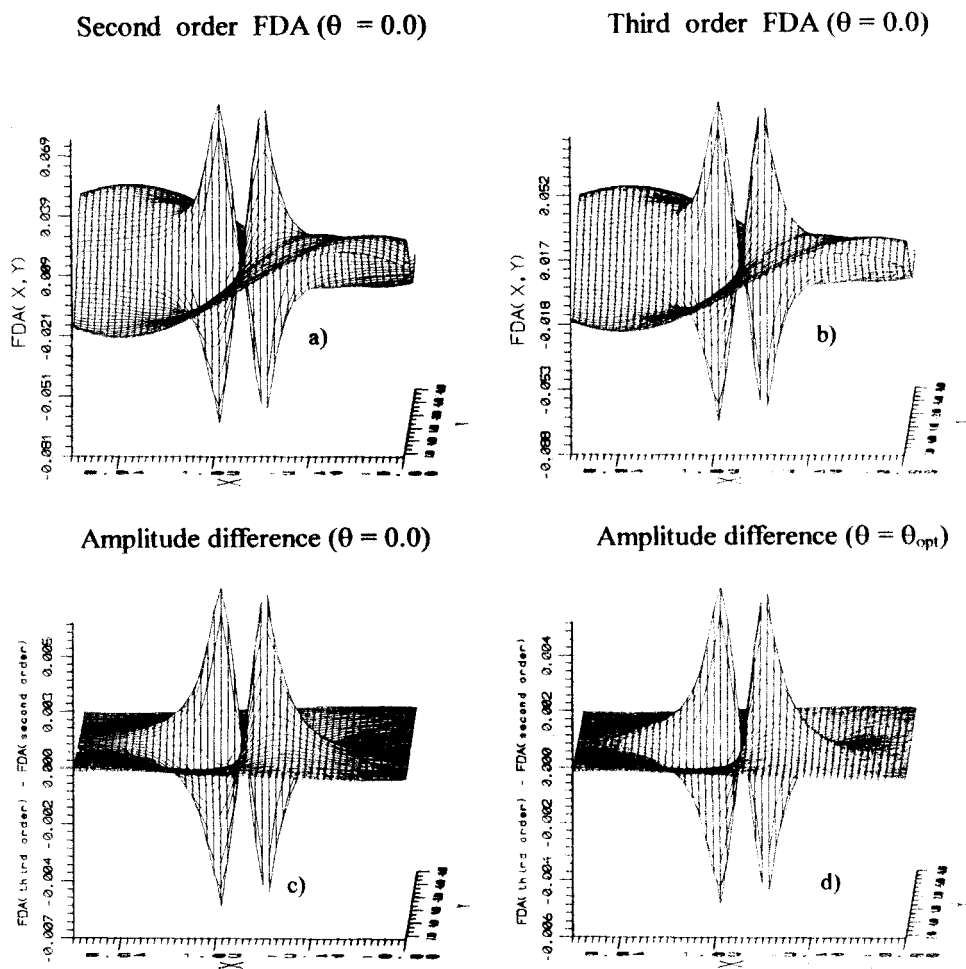


FIG. 4. The FDAs for  $\Sigma^2$ ,  $\Sigma^3$  and difference between the resonant FDAs from the second and third order decoupling at  $\theta=0.0$  and between the real parts at  $\theta=\theta_{\text{opt}}$  for  ${}^2\Pi_g N_2^-$  shape resonance are plotted in (a), (b), (c), and (d), respectively.

compared to that from  $\Sigma^2$  decoupling both at  $\theta=0.0$  and  $\theta=\theta_{\text{opt}}$  with redistribution at  $\theta_{\text{opt}}$  reinforcing the  $\pi^*$  character of the resonant FDA. These delicate variations in the resonant FDA attributes show that while the energetics may be described just as well by the  $\Sigma^2$  decoupling, the FDAs obtained from  $\Sigma^3$  decoupling have slightly larger electron amplitude at both C and O atoms which differ from each other at  $\theta=0.0$  and  $\theta=\theta_{\text{opt}}$  and if used as correlated LUMOs may

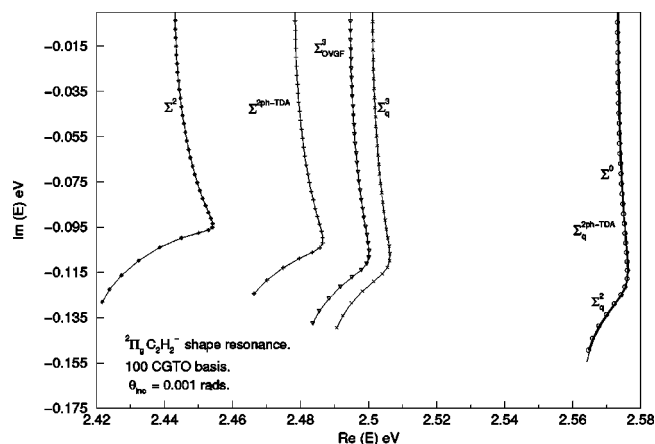


FIG. 5. Theta trajectories from different decouplings of dilated electron propagator on the  ${}^2\Pi_g C_2H_2^-$  shape resonance. The trajectories start on the real line ( $\theta=0.0$ ) and  $\theta$  increments are in steps of 0.001 rad.

TABLE III. Energy and width of the  ${}^2\Pi_g C_2H_2^-$  shape resonance.

| Method/Reference  | Energy (eV)    | Width (eV) |
|---|----------------|------------|
| Experiment:   |                |            |
| Vibrational excitation <sup>a</sup>   | 2.6            | >1.0       |
| Electron impact <sup>b</sup>  | 2.5            | ...        |
| Trapped electron <sup>c</sup>   | 1.8/1.85       | ...        |
| Dissociative attachment <sup>d</sup>  | $2.94 \pm 0.1$ | ...        |
| Theoretical approaches:   |                |            |
| Multiple-scattering $X\alpha^e$   | 2.6            | 1.0        |
| MNDO <sup>f</sup>   | 1.7–2.2        | ...        |
| CI <sup>g</sup>   | 3.29/2.92      | 1.1/1.1    |
| Results from bi-orthogonal dilated Electron propagator (this work):                       |                |            |
| Zeroth order ( $\Sigma^0$ ), quasiparticle  | 2.58           | 0.23       |
| Second order ( $\Sigma_q^2$ ) and quasiparticle   |                |            |
| Diagonal 2ph-TDA ( $\Sigma_q^{2\text{ph-TDA}}$ )  | 2.46           | 0.19       |
| Second order ( $\Sigma^2$ )   | 2.49           | 0.20       |
| Diagonal 2ph-TDA ( $\Sigma_q^{2\text{ph-TDA}}$ )  | 2.51           | 0.21       |
| Quasi-particle third order ( $\Sigma_q^3$ )   | 2.50           | 0.21       |
| OVGF third order ( $\Sigma_{\text{OVGF}}^3$ ) and third order ( $\Sigma^3$ ) <sup>h</sup> |                |            |

<sup>a</sup>Reference 30.

<sup>b</sup>Reference 34.

<sup>c</sup>References 35 and 36.

<sup>d</sup>Reference 37.

<sup>e</sup>Reference 31.

<sup>f</sup>Reference 32.

<sup>g</sup>Reference 33.

<sup>h</sup>Single point  $\Sigma^3(\eta, E)$  calculation for  $\eta = \eta_{\text{opt}}^q$  and  $E = E_{\text{res}}^q$  obtained from the  $\Sigma_q^3$  calculation.

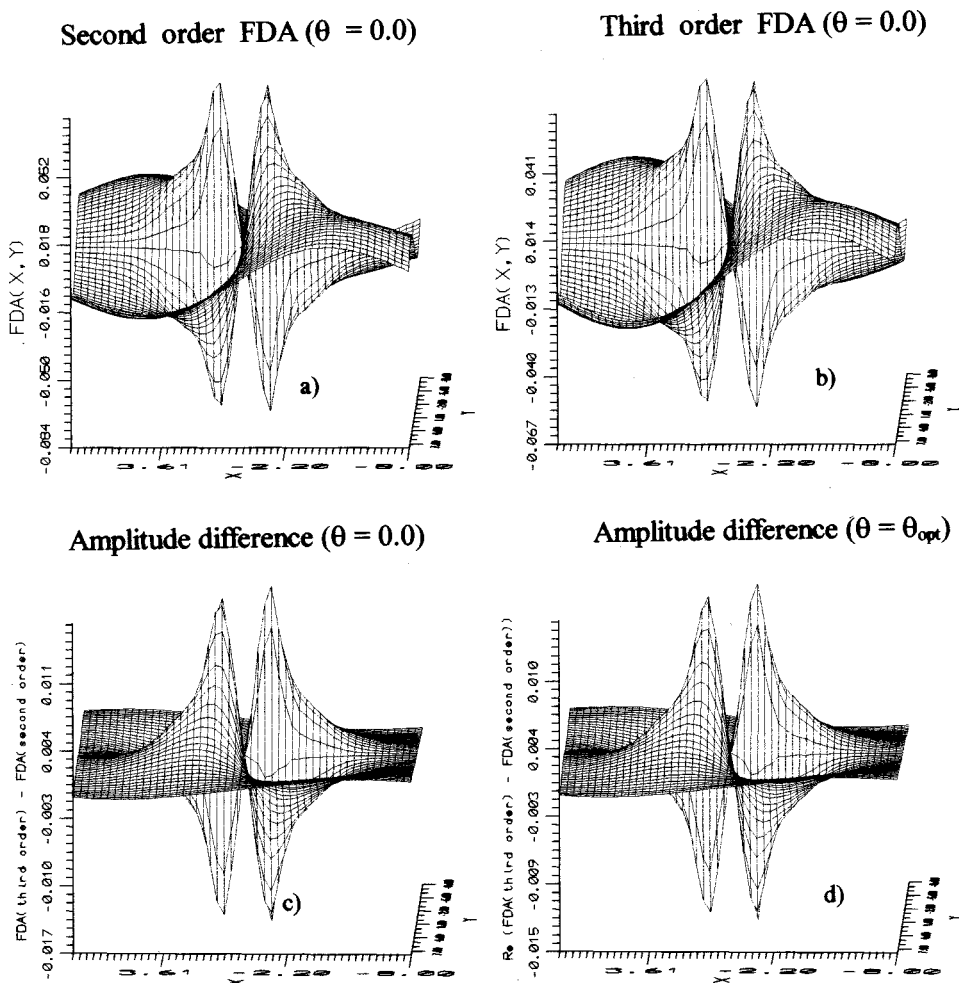


FIG. 6. The FDAs for  $\Sigma^2$ ,  $\Sigma^3$  and difference between the resonant FDAs from the second and third order decoupling at  $\theta=0.0$  and between the real parts at  $\theta=\theta_{\text{opt}}$  for  ${}^2\Pi_g \text{C}_2\text{H}_2^-$  shape resonance are plotted in (a), (b), (c), and (d), respectively.

provide superior description of other properties which are more sensitive to the wave function attributes.

### B. The ${}^2\Pi_g \text{N}_2^-$ shape resonance

The basis set effects for the  ${}^2\Pi_g \text{N}_2^-$  shape resonance were studied earlier<sup>53,54</sup> and the economic yet effective  $4s9p$  basis set used therein has been utilized again for testing the effectiveness of the new  $\Sigma_{\text{OVGF}}^3$ ,  $\Sigma_q^3$ ,  $\Sigma^3$ , and  $\tilde{\Sigma}^3$  decouplings. The theta trajectories from different decouplings using this basis are plotted in Fig. 3. Just as for the  $e$ -CO resonance (Fig. 1), the  $e$ - $\text{N}_2$  theta trajectories from the different third order decouplings are very close to those from second order decouplings. The energy and width obtained from the real and imaginary parts of the quasistable region of these trajectories along with those from experiment and other theoretical methods are collected in Table II. The quasiparticle decouplings are once again just as effective as their full nondiagonal counterparts and as seen earlier for the  ${}^2\Pi \text{CO}^-$ , the results obtained from full third order calculation are identical to those obtained from the  $\tilde{\Sigma}^3$  decoupling. The resonance energy for all the decouplings agree with the experimental values quite closely but the width from different decouplings are almost identical and much narrower in comparison to experimental and other computed values.

The third order decouplings are also examined by plotting the resonant FDAs at  $\theta=0.0$  and  $\theta=\theta_{\text{opt}}$  for both the  $\Sigma^2$

and the  $\Sigma^3$  decouplings. These have the typical  $\pi_g^*$  character of the  $\text{N}_2$  LUMO. The amplitude difference between second and third order decouplings at  $\theta=0.0$  and  $\theta=\theta_{\text{opt}}$  are displayed in Figs. 4(c) and 4(d). The  $\Sigma^3$  FDA once again provides for larger electron amplitude accumulation compared to  $\Sigma^2$  for both CO and  $\text{N}_2$ .

### C. The ${}^2\Pi_g \text{C}_2\text{H}_2^-$ shape resonance

The 100 CGTO basis with a  $5s9p1d$  CGTO basis on each C atom and a  $3s3p$  CGTO basis on each H atom used in our previous second order calculation<sup>29</sup> was employed again for investigating the  ${}^2\Pi_g \text{C}_2\text{H}_2^-$  shape resonance using third order decouplings. Theta trajectories from various third order decouplings of the dilated electron propagator utilizing this basis are plotted in Fig. 5. Resonance energies and widths are collected along with those obtained from other experimental and theoretical approaches in Table III. The results collected in Table III show that the resonance energies obtained using the  $\Sigma_{\text{OVGF}}^3$ ,  $\Sigma_q^3$ , and  $\Sigma^3$  decouplings are in excellent agreement with those obtained by more recent experiments<sup>30,34</sup> and the second order and diagonal 2ph-TDA results reported in our previous calculation.<sup>29</sup> The widths obtained using the third order decoupling are however much narrower in comparison with the only available experimental value<sup>30</sup> and are similar to those obtained using second order decouplings.<sup>29</sup>

The resonant FDAs obtained from second and third order decouplings at  $\theta=0.0$  are plotted in Figs. 6(a) and 6(b), respectively, and have a textbook outline of the simple  $\pi_g^*$  acetylene LUMO. Figures 6(c) and 6(d) show the difference between FDAs from second and third order decouplings. There is an overall relaxation of electron density around the C atoms brought out by the  $\Sigma^3$  decoupling and hence the resonance energy obtained using the third order is slightly higher than that obtained using the second order decoupling. That the electron density gets redistributed shows that third order decoupling does provide for additional electron correlation and relaxation in comparison to the second order decoupling. In order to understand the effect of complex scaling, the amplitude difference using second and third order decouplings at  $\eta = \eta_{\text{opt}}$  is displayed in Fig. 6(d). The amplitude difference profiles of Figs. 6(c) and 6(d) are very similar since  $\eta_{\text{opt}}$  ( $\alpha_{\text{opt}}=1.005$ ,  $\theta_{\text{opt}}=0.027$  rad,  $\eta = \alpha e^{i\theta}$ ) is very close to 1.0. Proximity of the optimal radial scale factor  $\alpha_{\text{opt}}$  to 1.0 points to the relative adequacy of the primitive basis and that  $\eta_{\text{opt}} \cong 1.0$  signifies an uncovering of the  ${}^2\Pi_g C_2H_2^-$  without too much distortion of the acetylene  $\pi_g^*$  orbital. This bolsters the prevalent view of the  ${}^2\Pi_g C_2H_2^-$  shape resonance being formed by a simple metastable trapping of the incident electron in the  $C_2H_2 \pi_g^*$  LUMO without much disturbance to and mixing with the rest of the target orbitals.

The lack of agreement between the calculated ( $\Sigma^3$ ) and the experimental width for this and the  ${}^2\Pi CO^-$  and  ${}^2\Pi_g N_2^-$  resonances even at the full  $\Sigma^3$  level leads us to infer that this may perhaps be due to lack of adequate static correlation in our calculations and a simple bivariational complex MCSCF may be required to provide a more suitable reference state.

#### IV. CONCLUDING REMARKS

The outer valence Green's function ( $\Sigma_{\text{OVGF}}^3$ ), quasiparticle third order ( $\Sigma_q^3$ ) and full third order ( $\Sigma^3$ ) decouplings of the bi-orthogonal dilated electron propagator have been developed and tested for the first time for molecular resonances by applying these decouplings to investigate the  ${}^2\Pi CO^-$ ,  ${}^2\Pi_g N_2^-$ , and  ${}^2\Pi_g C_2H_2^-$  shape resonances. The resonance energies and widths obtained using the third and the second order decouplings are close to each other and to those obtained from the zeroth order (bivariational SCF) decoupling. We are therefore led to believe that the  ${}^2\Pi CO^-$ ,  ${}^2\Pi_g N_2^-$ , and  ${}^2\Pi_g C_2H_2^-$  shape resonances do indeed conform to the classic picture of shape resonances resulting from a simple temporary attachment of the impinging electron into the target LUMO without much disturbance in terms of correlation with and relaxation of other electrons in the system. As seen here, the much more demanding  $\Sigma^3$ ,  $\Sigma_q^3$ , and  $\Sigma_{\text{OVGF}}^3$  decouplings may not offer much improvement in such cases. Both for  $\Sigma^2$  and  $\Sigma^3$  decouplings, the economic quasiparticle decouplings ( $\sim n^2/2$  times less demanding) provide almost identical results as far as the energetics of resonances are concerned.

One of the primary motives for the development of these methods was also to provide a rigorous characterization of LUMOs as resonant FDAs of the dilated electron propagator

and the techniques developed here do identify the resonant FDA as the correlated LUMO. The  $\Sigma^3$  decoupling provides for larger electron amplitude on both atoms of the diatomics CO and  $N_2$  investigated here. The  $\Sigma^3$  decoupling also provides for redistribution of electron amplitude on both C atoms in  $C_2H_2$ . The  $\Sigma^3$  decoupling may therefore be offering an improved description which is not tested sensitively enough by the energetic considerations alone. More applications to other molecular resonances and use of the resonant FDAs as correlated LUMOs in reactivity indices,<sup>59</sup> etc. alone can settle this issue. Also, as mentioned earlier, lack of agreement between the calculated and experimental width even with  $\Sigma^3$  decouplings may be a pointer to lack of adequate static correlation and a simple bivariational complex MCSCF may be required to provide a more suitable reference state. An effort along these lines is underway in our group.

#### ACKNOWLEDGMENT

The authors acknowledge financial support from the Department of Science and Technology, India (Grant No. SP/S1/H26/96).

- <sup>1</sup>J. Linderberg and Y. Öhrn, *Propagators in Quantum Chemistry* (Academic, New York, 1973).
- <sup>2</sup>P. Jorgensen and J. Simons, *Second Quantization Based Methods in Quantum Chemistry* (Academic, New York, 1981).
- <sup>3</sup>L. S. Cederbaum and W. Domcke, *Adv. Chem. Phys.* **36**, 205 (1977).
- <sup>4</sup>J. Simons, *Annu. Rev. Phys. Chem.* **28**, 15 (1977).
- <sup>5</sup>Y. Öhrn and G. Born, *Adv. Quantum Chem.* **13**, 1 (1981).
- <sup>6</sup>M. F. Herman, K. F. Freed, and D. L. Yeager, *Adv. Chem. Phys.* **48**, 1 (1981).
- <sup>7</sup>W. von Niessen, J. Schirmer, and L. S. Cederbaum, *Comput. Phys. Rep.* **1**, 57 (1984).
- <sup>8</sup>J. V. Ortiz, *Adv. Quantum Chem.* **35**, 33 (1999).
- <sup>9</sup>J. Aguilar, and J. Combes, *Commun. Math. Phys.* **22**, 269 (1971); E. Balslev and J. Combes, *ibid.* **22**, 280 (1971).
- <sup>10</sup>W. P. Reinhardt, *Annu. Rev. Phys. Chem.* **33**, 223 (1982).
- <sup>11</sup>B. R. Junker, *Adv. At. Mol. Phys.* **18**, 207 (1982).
- <sup>12</sup>P. Winkler, *Z. Phys. A* **291**, 199 (1977).
- <sup>13</sup>R. A. Donnelly and J. Simons, *J. Chem. Phys.* **73**, 2858 (1980).
- <sup>14</sup>M. Mishra, P. Froelich, and Y. Öhrn, *Chem. Phys. Lett.* **81**, 339 (1981).
- <sup>15</sup>M. K. Mishra and M. N. Medikeri, *Adv. Quantum Chem.* **27**, 223 (1996).
- <sup>16</sup>N. Moiseyev, S. Friedland, and P. R. Certain, *J. Chem. Phys.* **74**, 4739 (1981).
- <sup>17</sup>A. Venkatnathan, S. Mahalakshmi, and M. K. Mishra, *J. Chem. Phys.* **114**, 35 (2001).
- <sup>18</sup>G. J. Schulz, *Rev. Mod. Phys.* **45**, 379 (1970).
- <sup>19</sup>M. Zubek and C. Szmytkowski, *J. Phys. B* **10**, L27 (1977).
- <sup>20</sup>D. A. Levin, A. W. Fliflet, and V. McKoy, *Phys. Rev. A* **21**, 1202 (1980).
- <sup>21</sup>N. Chandra, *Phys. Rev. A* **16**, 80 (1977).
- <sup>22</sup>H. Erhardt, L. Langhans, F. Linder, and H. S. Taylor, *Phys. Rev.* **173**, 222 (1968).
- <sup>23</sup>B. I. Schneider, *Phys. Rev. A* **24**, 1 (1981).
- <sup>24</sup>B. I. Schneider, M. Le Dourneuf, and Vo Ky Lan, *Phys. Rev. Lett.* **43**, 1926 (1979).
- <sup>25</sup>J. S.-Y. Chao, M. F. Falcetta, and K. D. Jordan, *J. Chem. Phys.* **93**, 1125 (1990).
- <sup>26</sup>M. Krauss and F. H. Mies, *Phys. Rev. A* **1**, 1592 (1974).
- <sup>27</sup>M. Berman, O. Walter, and L. S. Cederbaum, *Phys. Rev. Lett.* **50**, 1979 (1983).
- <sup>28</sup>H. D. Meyer, *Phys. Rev. A* **40**, 5605 (1989).
- <sup>29</sup>A. Venkatnathan and M. K. Mishra, *Chem. Phys. Lett.* **296**, 223 (1998).
- <sup>30</sup>K. H. Kochem, W. Sohn, K. Jung, H. Erhardt, and E. S. Chang, *J. Phys. B* **18**, 1253 (1985).
- <sup>31</sup>J. A. Tossel, *J. Phys. B* **18**, 387 (1985).
- <sup>32</sup>J. Chandrasekhar, R. A. Kahn, and P. R. Schleyer, *Chem. Phys. Lett.* **85**, 493 (1982).

- <sup>33</sup>V. Krumbach, B. M. Nestmann, and S. D. Peyerimhoff, *J. Phys. B* **22**, 4001 (1989).
- <sup>34</sup>L. Andric and R. I. Hall, *J. Phys. B* **21**, 355 (1988).
- <sup>35</sup>D. F. Dance and I. C. Walker, *Chem. Phys. Lett.* **18**, 601 (1973).
- <sup>36</sup>E. H. Van Veen and F. L. Plantenga, *Chem. Phys. Lett.* **38**, 493 (1976).
- <sup>37</sup>R. Dressler and H. Allan, *J. Chem. Phys.* **87**, 4510 (1987).
- <sup>38</sup>M. Mishra, Y. Öhrn, and P. Froelich, *Phys. Lett. A* **84**, 4 (1981).
- <sup>39</sup>R. Manne, *Chem. Phys. Lett.* **45**, 470 (1977).
- <sup>40</sup>E. Dalgaard, *Int. J. Quantum Chem.* **15**, 169 (1979).
- <sup>41</sup>O. Gosinski and B. Lukman, *Chem. Phys. Lett.* **7**, 573 (1970).
- <sup>42</sup>R. Longo, B. Champagne, and Y. Öhrn, *Theor. Chim. Acta* **90**, 397 (1995).
- <sup>43</sup>P. O. Löwdin, P. Froelich, and M. Mishra, *Adv. Quantum Chem.* **20**, 185 (1989).
- <sup>44</sup>J. Schirmer and L. S. Cederbaum, *J. Phys. B* **11**, 1889 (1978); **11**, 1901 (1978).
- <sup>45</sup>G. Born and Y. Öhrn, *Chem. Phys. Lett.* **61**, 397 (1979).
- <sup>46</sup>M. N. Medikeri, J. Nair, and M. K. Mishra, *J. Chem. Phys.* **99**, 1869 (1993).
- <sup>47</sup>J. V. Ortiz, *Int. J. Quantum Chem., Symp.* **S22**, 431 (1988).
- <sup>48</sup>L. S. Cederbaum, *Theor. Chim. Acta* **31**, 239 (1973).
- <sup>49</sup>M. N. Medikeri and M. K. Mishra, *Chem. Phys. Lett.* **211**, 607 (1993).
- <sup>50</sup>R. A. Donnelly, *Int. J. Quantum Chem., Symp.* **S19**, 337 (1985).
- <sup>51</sup>M. N. Medikeri and M. K. Mishra, *J. Chem. Phys.* **103**, 676 (1995).
- <sup>52</sup>J. V. Ortiz, *Chem. Phys. Lett.* **216**, 319 (1993); **199**, 530 (1992).
- <sup>53</sup>S. Mahalakshmi and M. K. Mishra, *Indian J. Chem.* **39A**, 22 (2000).
- <sup>54</sup>M. N. Medikeri and M. K. Mishra, *Int. J. Quantum Chem., Symp.* **S28**, 29 (1994).
- <sup>55</sup>L. Dube and A. Herzenberg, *Phys. Rev. A* **20**, 194 (1979).
- <sup>56</sup>A. U. Hazi, T. N. Rescigno, and M. Kurilla, *Phys. Rev. A* **23**, 1089 (1981).
- <sup>57</sup>T. N. Rescigno, A. E. Orel, and C. W. McCurdy, *J. Chem. Phys.* **73**, 6347 (1980).
- <sup>58</sup>R. A. Donnelly, *Int. J. Quantum Chem., Symp.* **S16**, 653 (1982).
- <sup>59</sup>I. Fleming, *Frontier Orbitals and Organic Chemical Reactions* (Wiley, Chichester, 1978).